Uptake and metabolic fate of [His^{A8},His^{B4},Glu^{B10},His^{B27}]insulin in rat liver *in vivo*

François AUTHIER*[1], Gianni M. Di GUGLIELMO†, Gillian M. DANIELSEN‡ and John J. M. BERGERON†

*Institut National de la Santé et de la Recherche Médicale U30, Hôpital Necker des Enfants Malades, 75015 Paris, France, †Anatomy and Cell Biology, McGill University, Montreal, Québec H3A 2B2, Canada, and ‡Health Care Discovery, Novo Nordisk A/S, Novo Alle, DK-2880 Bagsvaerd, Denmark

Receptor-mediated endocytosis and subsequent endosomal proteolysis of [^{125}I]Tyr^{A14}-[His^{A8},His^{B4},Glu^{B10},His^{B27}]insulin ([^{125}I]Tyr^{A14}-H2 analogue), an insulin analogue exhibiting a high affinity for the insulin receptor, has been studied in liver parenchymal cells by quantitative subcellular fractionation and compared with that of wild-type [^{125}I]Tyr^{A14}-insulin. Whereas the kinetics of uptake of the H2 analogue by liver was not different from that of insulin, the H2 analogue radioactivity after the 2 min peak declined significantly more slowly. A significant retention of the H2 analogue compared with insulin in both plasma membrane and endosomal fractions was observed and corresponded to decreased processing and dissociation of the H2 analogue. Cell-free endosomes preloaded *in vivo* with radiolabelled ligands and incubated *in vitro* processed insulin and extraluminally released insulin intermediates at a 2–3-fold higher rate than the H2 analogue. *In vitro* proteolysis of both non-radiolabelled and monoiodinated molecules by endosomal lysates showed a decreased response to the endosomal proteolytic machinery for the H2 analogue. However, in cross-linking and competition studies the H2 analogue exhibited an affinity for insulin-degrading enzyme identical with that of wild-type insulin. Brij-35-permeabilized endosomes revealed a 2-fold higher rate of dissociation of insulin from internalized receptors compared with the H2 analogue. After the administration of a saturating dose of both ligands, a rapid and reversible ligand-induced translocation of insulin receptor was observed, but without receptor loss. The H2 analogue induced a higher receptor concentration and tyrosine autophosphorylation of the receptor β subunit in endosomes. Moreover, a prolonged temporal interaction of the *in vivo* injected H2 analogue with receptor was observed by direct binding assays performed on freshly prepared subcellular fractions. These results indicate that endosomal proteolysis for the H2 analogue is slowed as a result of an increased residence time of the analogue on the insulin receptor and a low affinity of endosomal acidic insulinase for the dissociated H2 molecule.

INTRODUCTION

Insulin degradation in liver parenchymal cells has been shown to be a consequence of receptor-mediated endocytosis [1]. Concomitant with, or shortly after, receptor activation at the plasma membrane level, the insulin–receptor complex undergoes endocytosis into an acidic compartment where the termination of the insulin signal occurs by two independent processes [2,3]. Endosomal proteolysis of the ligand is required for the prevention of continual stimulation of autophosphorylation [2–4]. Endosomal dephosphorylation then leads to the deactivation of the receptor's exogenous kinase activity [5].

Evidence of a role for hepatic endosomes in the degradation of internalized insulin comes from a variety of results: (1) cell fractionation studies yielded a high recovery of internalized insulin in purified endosomes with little hormone observed in lysosomes both for rat liver parenchyma [6,7] and hepatoma Fao cells [8]; (2) inhibitors of lysosomal proteases do not modify endosomal insulin degradation in cell-free endosomes [9–11], in hepatoma cell lines [8] and by the relevant endosomal insulinase activity [4]; (3) intact as well as degraded insulin was identified in endosomal fractions isolated at various stages of endocytosis [6–12]; (4) isolated intact endosomes were shown to degrade previously internalized insulin [9–12]; and (5) a thiol-dependent rat liver endosomal acidic insulinase with a partial metal ion requirement has been partly characterized [4].

Endosomal acidic insulinase, which has been suggested to display a restricted expression in insulin-sensitive tissues [8], is not related to insulin-degrading enzyme (IDE), previously reported to be a candidate for the hydrolysis of internalized insulin [2,4], nor to the acidic glucagon-degrading activity of hepatic endosomes that has been attributed to membrane-bound forms of cathepsins B and D [13]. The endosomal degradation of insulin results in a clipped insulin molecule that can no longer bind to its receptor within endocytic structures [12]. Although some cleavage sites of insulin produced by rat hepatic endosomal insulinase activity have been identified [12], little is known about the regions of the insulin molecule that are responsible for selective binding to endosomal acidic insulinase. The identification of such residues would facilitate the design of protease-resistant insulin analogues. However, because insulin-specific receptors also mediate insulin removal from the extracellular space, then a feature relevant to the development of such protease-resistant insulin analogues is to preserve receptor-binding capacity while altering protease affinity. Considerable details are known about the increase in binding affinity and the metabolic and mitogenic potencies of numerous low-K_d analogues such as [Asp^{B10}]insulin and [His^{A8},His^{B4},Glu^{B10},His^{B27}]insulin (H2 analogue) [14–16]. However, few studies have been directed towards the cell-mediated metabolism of these molecules; in particular the roles of receptor-mediated endocytosis and subsequent endosomal degradation in defining their degradation pathway remain undefined.

The object of the present study was to investigate the uptake and subsequent metabolic fate of the H2 analogue (which displays the slowest dissociation rate constant [15]) and to compare them

Abbreviations used: BS^3, bis(sulphosuccinimidyl)suberate; DSS, disuccinimidyl suberate; EGF, epidermal growth factor; H2 analogue, [His^{A8},His^{B4},Glu^{B10},His^{B27}]insulin; HRP, horseradish peroxidase; IDE, insulin-degrading enzyme; PEG, poly(ethylene glycol); SEE, soluble endosomal extract.

[1] To whom correspondence should be addressed.

with those of wild-type insulin by using the quantitative subcellular fractionation of rat liver. We demonstrate a decreased ability for the H2 analogue to dissociate from the insulin receptor and to be subsequently proteolysed by endosomal acidic insulinase within the endosomal lumen. In contrast the enzyme known previously as IDE was unable to distinguish between insulin and the H2 analogue. Finally we report on the effect of ligand occupancy *in vivo* on the kinetics and extent of insulin receptor internalization. Our results show that, compared with insulin, the H2 analogue treatment resulted in a higher extent and duration of (1) insulin receptor occupancy by administered ligand in the whole-liver parenchymal cell; (2) insulin receptor internalization into endocytic components; and (3) tyrosine phosphorylation of the insulin receptor β subunit within endosomal fractions.

EXPERIMENTAL

Protein determination, antibodies and materials

Total protein was determined by the method of Lowry et al. [17]. Monoclonal antibody directed against the human IDE [18] was a gift from Dr. R. A. Roth (Stanford University, Stanford, CA, USA). Polyclonal IgG against the human insulin receptor β subunit was purchased from UBI. Monoclonal horseradish peroxidase (HRP)-conjugated antibody raised against phosphotyrosine was purchased from Amersham. HRP-conjugated goat anti-(rabbit IgG) was from Bio-Rad. H2 analogue was produced and purified as described previously [16]. Human insulin (used as the reference insulin) was purchased from Sigma. Bis(sulphosuccinimidyl)suberate (BS^3) and disuccinimidyl suberate (DSS) were purchased from Pierce. All other chemicals were obtained from commercial sources and were of reagent grade.

Animals and injections

Male Sprague–Dawley rats weighing 180–200 g were obtained from Charles River (St. Aubin Les Elbeufs, France) and were fasted for 18 h before being killed. [^{125}I]Tyr^{A14}-labelled ligands (30×10^6 c.p.m., approx. 9 pmol) or native ligands (15 μg/100 g body weight) were diluted in 0.3 ml of 0.15 M NaCl and injected within 5 s into the penis vein under light anaesthesia with ether. In studies with native ligands, saline-injected rats were used as controls.

Preparation of [^{125}I]Tyr^{A14}-labelled ligands

Human insulin and the H2 analogue were radioiodinated by the lactoperoxidase method as described previously [15,19] to specific activities of 350–380 μCi/μg. The iodinated mixture was immediately loaded on a reverse-phase HPLC column (Waters μBondapak C_{18}, 0.39 cm $\times$ 30 cm, 10 μm particle size) and chromatographed with a mixture of 0.1 % (v/v) trifluoroacetic acid in water (solvent A) and 0.1 % (v/v) trifluoroacetic acid in acetonitrile (solvent B) as eluent, at a flow rate of 2 ml/min. Elution was performed by isocratic elution of 30 % solvent B. Eluates were monitored on-line for absorbance at 280 nm with an LC spectrophotometer and for radioactivity with a Berthold LB 504 γ-detector connected to an Apple IIe computer. The major components in the eluates (peaks II and IV; see Figure 1) were collected and freeze-dried. To ensure identity of the radiolabelled tyrosine residue in the H2 analogue molecule, a mixture of peak IV (2×10^6 c.p.m.) and approx. 300 pmol of native H2 analogue was subjected to N-terminal sequence analysis with an Applied Biosystems model 476A analyser in accordance with methods described previously [19,20].

Isolation of subcellular fractions from rat liver

After injections, rats were killed; livers were removed rapidly and minced in either isotonic or hypotonic ice-cold homogenization buffer containing 20 mM Tris/HCl, pH 7.4, 1 mg/ml bacitracin, 5 mM 1,10-phenanthroline, 2 mM *N*-ethylmaleimide, 4 mM NaF and 100 μM Na_3VO_4. All subsequent steps were performed at 4 °C and all buffers contained the protease and phosphatase inhibitors stated above. A total particulate fraction was isolated from homogenates as reported [21]. Plasma membranes were prepared from homogenates in 1 mM bicarbonate by the method of Neville [22] up to step 11 [4,19,21]. The cytosolic fraction was isolated from homogenates in 0.25 M sucrose by differential centrifugation [4,13,19]. Endosomal fraction was isolated by discontinuous gradient centrifugation as described previously [4,13,19–21]. The soluble endosomal extract (SEE) was isolated by hypotonic shock as reported [4,13].

Assay for intra-endosomal degradation of [^{125}I]Tyr^{A14}-labelled ligands

Endosomal fraction isolated in the absence of protease inhibitors 4 min after the injection of [^{125}I]Tyr^{A14}-labelled ligands was suspended at 1 mg/ml in 0.15 M KCl containing 5 mM $MgCl_2$, 50 mM citrate phosphate buffer, pH 3–8.5, and, where indicated, 1 mM ATP. Samples were incubated at 37 °C for various periods, after which the integrity of the ligands was assessed by precipitation with trichloroacetic acid [4,13,19,20].

Assay for intra-endosomal dissociation of [^{125}I]Tyr^{A14}-labelled ligands

Dissociation of [^{125}I]Tyr^{A14}-labelled ligands from the endosomal insulin receptor was assessed by precipitation with poly(ethylene glycol) (PEG) in the absence or presence of the detergent Brij-35, as described in similar studies with insulin [9] and glucagon [20]. In intact endosomes, both receptor-bound and free intraluminal ligands are PEG-precipitable. In Brij-35-permeabilized endosomes, only receptor-bound ligands remain PEG-precipitable [9,20].

Ligand degradation assays

The radioactivity associated with cell fractions from [^{125}I]Tyr^{A14}-labelled ligand-injected rats was assayed by precipitation with trichloroacetic acid, as reported previously [19,20]. Degradation of the [^{125}I]Tyr^{A14}-labelled ligands *in vitro* by a SEE and the cytosolic fraction was measured by precipitation with trichloroacetic acid [4,13] and by reverse-phase HPLC. For the latter method, the samples were acidified with acetic acid (15 %, v/v) and immediately loaded on a μBondapak C_{18} HPLC column. Elution was performed by using two sequential linear gradients with the same solvents as described for the purification of native radiolabelled isomers: first, a gradient of 0–20 % (v/v) solvent B (15 min); secondly, a gradient of 20–45 % (v/v) solvent B (70 min). HPLC processing assays with unlabelled peptides were carried out by using the same gradients described above, with subsequent detection at 214 nm [13].

Cross-linking studies

Affinity-labelling of cytosolic IDE by radiolabelled insulin was performed by the method of Authier et al. [4,13,23] with BS^3 as cross-linker. In some experiments the cytosolic fraction was immunodepleted of IDE before the cross-linking procedure, as reported [4,13,23]. Affinity-labelling of endosomal insulin receptor by radiolabelled ligands was performed as described

above except that DSS was used as cross-linker instead of BS^3. Slab-gel electrophoresis [8% (w/v) polyacrylamide resolving gel] in the presence of SDS under reducing conditions was performed by the method of Laemmli [24].

Insulin receptor binding assays

Direct binding studies with [^{125}I]Tyr^{A14}-insulin were performed as described by Desbuquois et al. [25]. Before the binding assay, subcellular fractions from native ligand-injected rats were subjected to acid treatment to extract the insulin and H2 analogue molecules that remained bound to the insulin receptor. Isolated fractions (200 μg) were incubated in 500 μl of 60 mM citrate phosphate buffer, pH 4, containing 10 mg/ml BSA and 1 mg/ml bacitracin. After 30 min at 21 °C, the samples were centrifuged at 300000 ***g*** at 4 °C for 30 min. The resultant pellets were resuspended in 50 mM Tris/HCl, pH 7.4, and tested for [^{125}I]Tyr^{A14}-insulin-binding activity, as reported [25]. The effect of pH on the binding of [^{125}I]Tyr^{A14}-insulin or [^{125}I]Tyr^{A14}-H2 analogue to the intracellular endosomal insulin receptor was studied as described above except that 50 mM citrate phosphate buffer, pH 4–7.5, was used instead of Tris/HCl buffer, pH 7.4. The PEG precipitation method of Cuatrecasas [26] was used to separate free and receptor-bound ligands. The non-specific binding of ligands to cell membranes was less than 3% of the total radioactivity added.

Immunoblot studies

Samples after electrophoresis were transferred to nitrocellulose blots and immunoblotted as described by Authier et al. [4,13,27]. Antibodies raised against the insulin receptor and phosphotyrosine were used at dilutions of 1:2500 and 1:200 respectively. Bound immunoglobulin was detected with HRP-conjugated goat anti-(rabbit IgG) for the polyclonal anti-insulin receptor antibody.

RESULTS

We have investigated the metabolic fate of [^{125}I]Tyr^{A14}-insulin and [^{125}I]Tyr^{A14}-H2 analogue by quantitative subcellular fractionation of rat liver after the intravenous injection of radiolabelled ligands into rats. We have attempted to characterize biochemically both ligands associated with subcellular fractions throughout the internalization pathway by assessment of (1) their degree of integrity by precipitation with trichloroacetic acid and analysis by HPLC; (2) their degree of association with the insulin receptor by precipitation with PEG; (3) the effect of pH on their dissociation and degradation states within endosomes by using a cell-free system; and (4) the effect of ligand occupancy *in vivo* on the internalization and autophosphorylation of the insulin receptor.

Preparation of ^{125}I-labelled derivatives of insulin and the H2 analogue with defined structures

Because structural differences between the labelled hormones might significantly alter their interactions with the insulin receptor and/or insulin proteolytic activities, we first undertook to generate equivalently radioiodinated isomers. Figure 1(A) shows a typical HPLC profile resulting from the iodination of human insulin. Previous studies have shown that such an iodination protocol followed by reverse-phase HPLC purification resulted in a mixture of two products in which the A-chain tyrosines were independently derivatized [15]. The minor radioactive material (peak I; elution time 13 min) co-eluted with unlabelled insulin was identified as insulin monoiodinated in the Tyr^{A19} position, and the major radioactive product eluted last (peak II; elution time 27 min) was shown to represent [^{125}I]Tyr^{A14}-insulin [15]. A similar HPLC pattern was obtained after iodination of the H2 analogue (Figure 1B). An identical product (peak III; elution time 12 min) eluted before the unlabelled H2 analogue (elution time 13 min) was identified, whereas the major radioactive product (peak IV; elution time 26 min) was detected. Further characterization of the iodinated H2 analogue product IV was performed by radiosequence analysis (results not shown). Automated Edman degradation showed that radioactivity was released during the 14th cycle, confirming the identity of product IV as [^{125}I]Tyr^{A14}-H2 analogue.

Clearance of radiolabelled ligands from rat liver homogenates

Both ligands were retained in the liver, with a maximum retention of radiolabel at 2 min (Figure 2, upper panel). Both molecules were then cleared from the liver at approximately the same rates with a $t_{\frac{1}{2}}$ of approx. 14 min. The H2 analogue revealed a greater rate of accumulation at the maximum retention time of 2 min (approx. 23% and 19% of the dose per g of liver for the H2 analogue and insulin respectively) and a significantly longer retention over the further 30 min period compared with insulin. The integrity of ligands as assessed by precipitation with trichloroacetic acid revealed a time-dependent increase in degradation (Figure 2, lower panel). After 2 min the rate of insulin proteolysis exceeded that of the H2 analogue by 15–20%, with $t_{\frac{1}{2}}$ values for degradation of 22.6 and 39 min respectively.

The temporal relationship between endocytosis and degradation of radiolabelled ligands

Both ligands accumulated transiently in plasma membrane and endosomal fractions (Figure 3, upper panels). However, quantitative differences in the extent and rates of accumulation of the ligands into the subcellular fractions were observed. Ligand association with plasma membranes was 2–3-fold higher relative to the homogenate for the H2 analogue as compared with insulin, with relative specific activities of 10.4 and 4 respectively at the maximum time of association (30 s). This subcellular fraction also showed a significant difference in the rate of loss of the H2 analogue with a $t_{\frac{1}{2}}$ of approx. 34.7 s, whereas that of insulin was 70.5 s. A further difference in the handling of the ligands was observed in endosomal fractions. The rate of uptake into endosomes was faster for the H2 analogue, with an enrichment of 71.6-fold at 2 min, compared with 52.4-fold for insulin. Whereas intraendosomal insulin declined rapidly, a temporal retention of the H2 analogue in endosomes was observed from 15 to 60 min, with a considerably higher enrichment at 15 min (100.4-fold for the H2 analogue compared with 41.0-fold for insulin).

On the basis of the trichloroacetic acid-precipitation assay, at up to 2 min after injection both ligands that were associated with the plasma membranes remained largely intact (Figure 3, lower panels). The degradation of insulin then increased gradually over the next 6 min, 3-fold faster than that of the H2 analogue. Comparably, the amount of degraded insulin associated with endocytic structures increased progressively from 10% to 20% between 2 and 30 min, whereas that of the H2 analogue did not exceed 6% over the same times.

Cell-free degradation of radiolabelled ligands within isolated endosomes

Endosomal fractions containing previously internalized radiolabelled ligands were assayed for their ability to degrade the

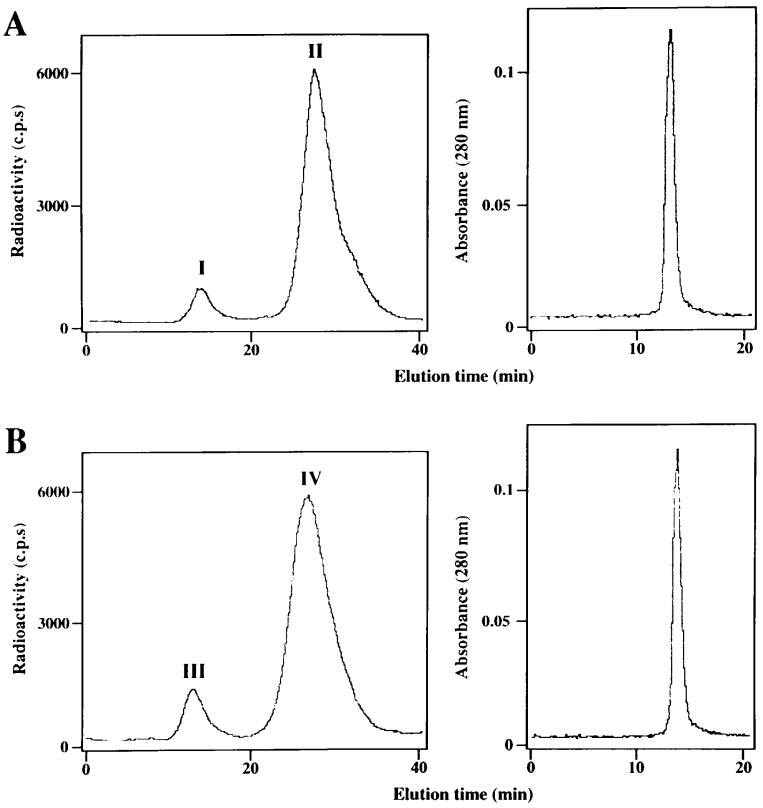

Figure 1 Reverse-phase HPLC purification of radioiodinated ligands

A lactoperoxidase-based iodination mixture of human insulin (**A**) or H2 analogue (**B**) was applied to a μBondapak C_{18} column. The HPLC profiles in the left panels plot radioactivity against elution time. Products II and IV were collected and freeze-dried. The HPLC profiles in the right panels represent absorbance analysis at 280 nm after injection into the column of unlabelled insulin and H2 analogue. The profiles shown are representative of seven experiments.

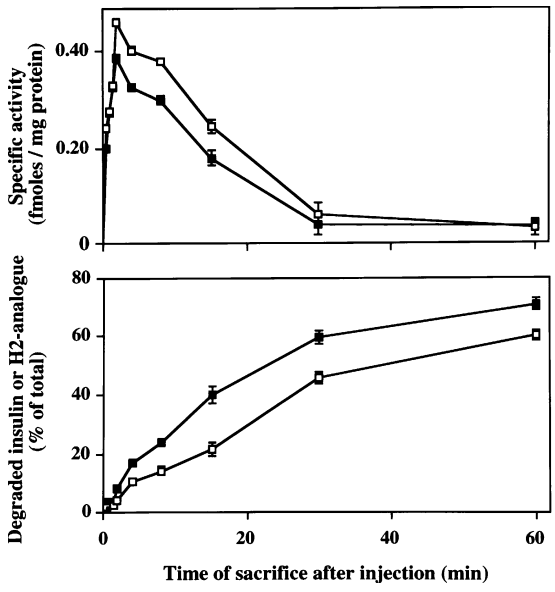

Figure 2 Kinetics of uptake and degradation of radiolabelled ligands in rat liver

Liver homogenates were prepared from rats killed at the indicated times after the administration of insulin (■) or H2 analogue (□). Recovered radioactivity in the homogenates was quantified (upper panel), and integrity was assessed by precipitation with trichloroacetic acid (lower panel). Each point is the mean ± S.D. for 12–15 separate experiments.

ligands *in vitro* (Figure 4). Degradation of insulin and the H2 analogue within endosomes was dependent on the medium pH and occurred mainly at pH 6 (Figure 4A). At any pH, cell-free endosomes processed insulin approx. 2–3-fold faster than they did the H2 analogue.

Endosomes decrease their internal pH via an ATP-driven proton pump [2,3,11,19,20]. We therefore also studied the sensitivity of ligand proteolysis in cell-free endosomes to ATP (Figure 4B). ATP shifted the pH for maximal ligand degradation to approx. 7 as expected [11], but the difference in the rates of degradation of the two ligands was still maintained.

Degradation of insulin and the H2 analogue by endosomal acidic insulinase

Endosomes were disrupted by hypotonic shock and the SEE from the 30 min centrifugation at 300000 ***g*** was assayed for its ability to proteolyse radiolabelled molecules at pH 5 and 37 °C by using HPLC (Figure 5A). A representative elution profile obtained after a 90 min incubation revealed more than 60 % of insulin degradation with a concomitant generation of major degradation products and mono[^{125}I]Tyr. With the H2 analogue as a substrate, the radioactivity was recovered mainly as an intact radiolabelled molecule along with the appearance of minor degradation products and mono[^{125}I]Tyr.

Studies were also performed with unmodified insulin and H2 analogue to exclude the potential confounding effects of radiolabelling (Figure 5B). Incubation of the SEE with intact insulin

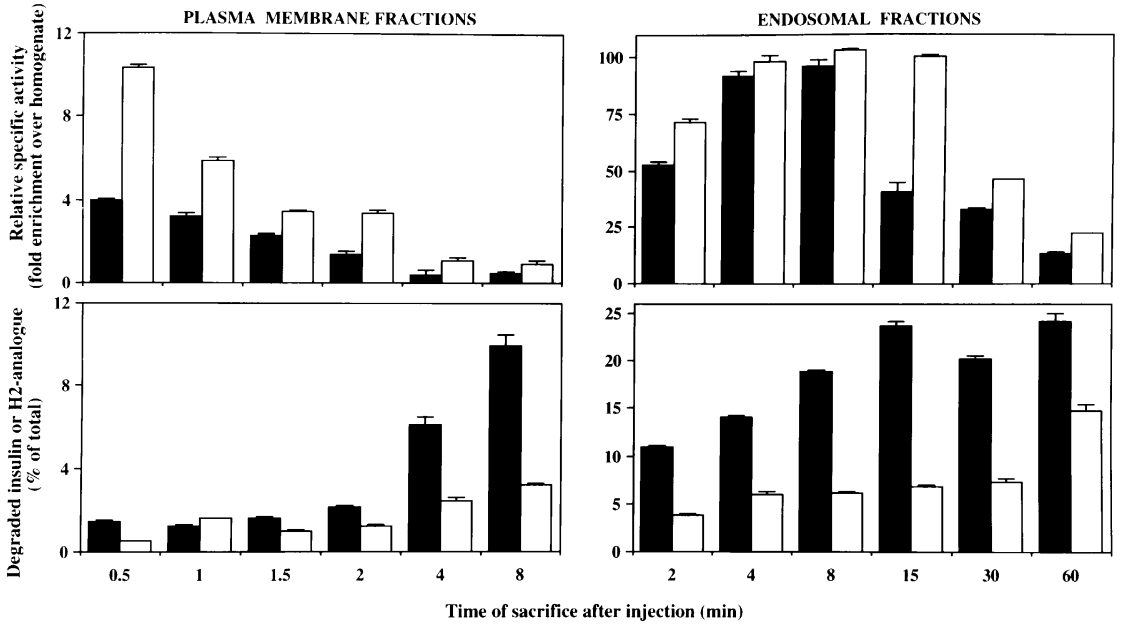

Figure 3 Kinetics of internalization of radiolabelled ligands in rat liver

Fractions of liver plasma membrane (left panels) and endosomes (right panels) were isolated from rats killed at the indicated times after the administration of insulin (filled bars) or H2 analogue (open bars). Upper panels: radioactivity associated with subcellular fractions was quantified and the enrichment of internalized ligands was expressed by reference to the radioactivity in the homogenates (relative specific activity). Lower panels: the amount of degraded ligand was determined by precipitation with trichloroacetic acid. The results are means ± S.D. from six to seven fractionations.

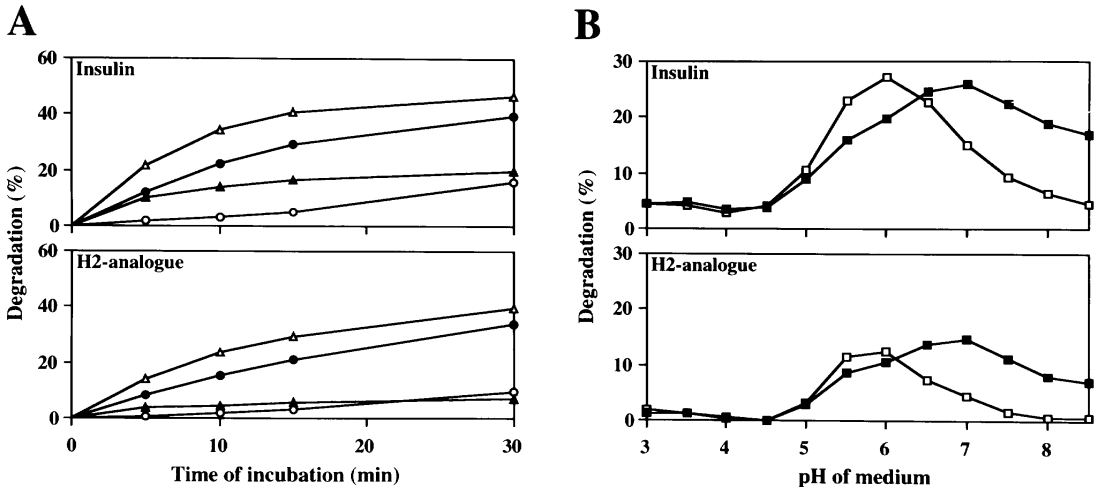

Figure 4 pH dependence of cell-free degradation of radiolabelled ligands within endosomes

Endosomal fractions were isolated from rats killed 4 min after the injection of radiolabelled ligands. (**A**) Endosomes were incubated for various lengths of time at pH 4 (○), 5 (▲), 6 (△) or 7 (●), after which the amount of degraded ligand was determined by precipitation with trichloroacetic acid. (**B**) Endosomes were incubated at different pH values for 5 min in the absence (□) or presence (■) of 1 mM ATP, after which the amount of degraded ligand was determined by precipitation with trichloroacetic acid.

resulted in a rapid generation of insulin peptide products with 80% proteolysis in 2 h. With the H2 analogue, less than 20% degradation was detected after the same incubation period.

Degradation of insulin and the H2 analogue by cytosolic IDE

IDE has been proposed to be physiologically relevant to the mechanism of insulin clearance from liver parenchymal cells [2,28,29]. We attempted to evaluate the relevance of cytosolic IDE to the differential processing of insulin and the H2 analogue by rat liver (Figure 6). With the trichloroacetic acid-precipitation assay (Figure 6A), each of the radiolabelled ligands approached steady states of degradation at the same rate, with 50% proteolysis obtained after approx. 15 min of incubation. To test further the relative catalytic selectivity of IDE towards both molecules, we evaluated the ability of the ligands to inhibit

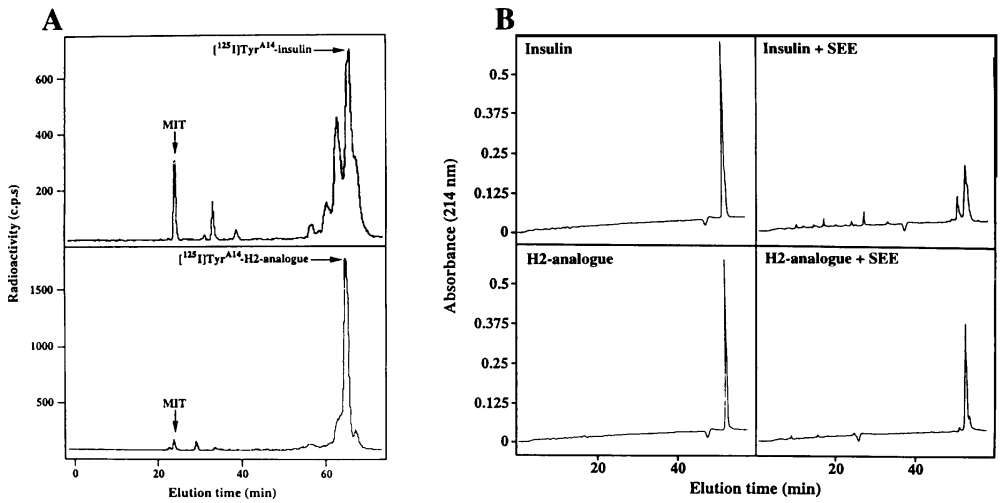

Figure 5 HPLC elution profiles of the degradation products resulting from the incubation of insulin and the H2 analogue with a SEE at acidic pH

Endosomes were disrupted by hypotonic shock, and the SEE was evaluated for its insulin- and H2 analogue-degrading activities at pH 5 and 37 °C. (**A**) The SEE was incubated with 500 fmol of radiolabelled ligand for 90 min. The proteolytic reaction was then stopped with acetic acid [15% (v/v) final concentration] and the incubation mixture was analysed by reverse-phase HPLC. The arrows indicate the elution time of intact [^{125}I]Tyr^{A14}-insulin (66 min), intact [^{125}I]Tyr^{A14}-H2 analogue (65 min) and free [^{125}I]Tyr (MIT; 24 min). The radioactivity corresponding to undegraded [^{125}I]Tyr^{A14} isomers was 2000 c.p.s. (**B**) The SEE was incubated with insulin or the H2 analogue (1 μM final concentration) for 2 h. The proteolytic reaction was then stopped with acetic acid [15% (v/v) final concentration] and the incubation mixture was analysed by reverse-phase HPLC. All panels in (**B**) show absorbance profiles at 214 nm. Intact insulin and H2 analogue had an elution time of 57 min. The endosomal proteins themselves did not give any detectable absorbance peak (results not shown).

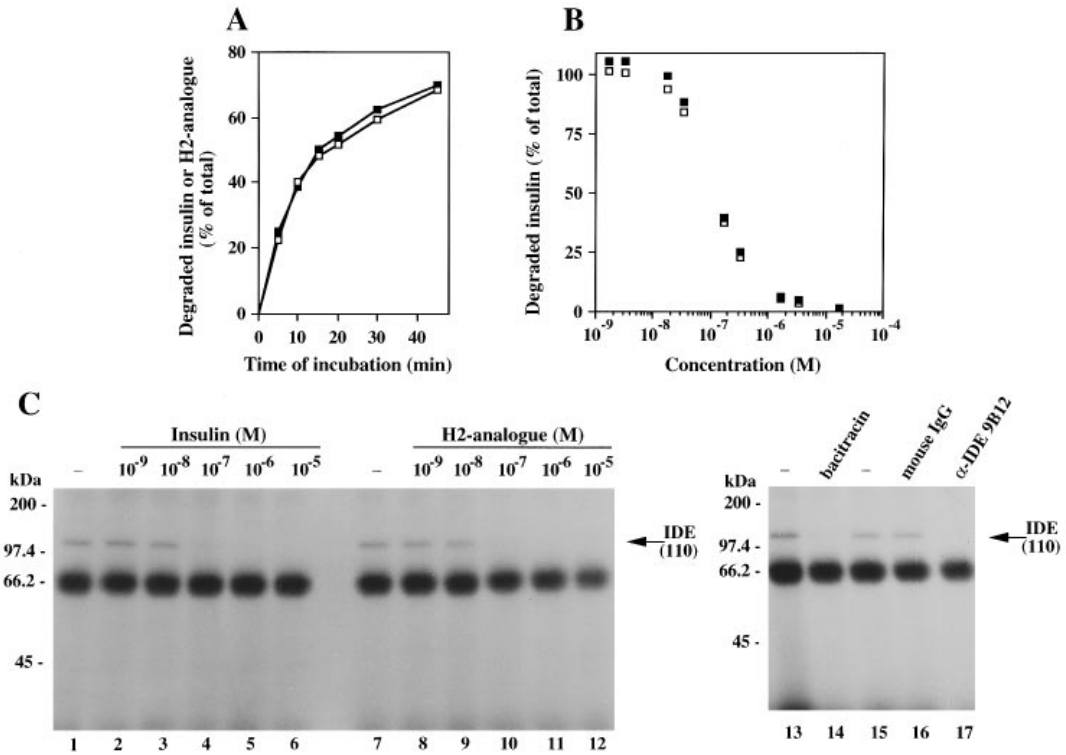

Figure 6 Assessment of the proteolysis of insulin and the H2 analogue by IDE

(**A**) The cytosolic fraction (0.1 mg/ml) was tested for its ability to degrade 50 fmol of [^{125}I]Tyr^{A14}-insulin (■) or [^{125}I]Tyr^{A14}-H2 analogue (□) at 37 °C and pH 7 by precipitation with trichloroacetic acid. (**B**) [^{125}I]Tyr^{A14}-insulin (50 fmol) and the cytosolic fraction (0.1 mg/ml) were incubated at 37 °C and pH 7 for 5 min with the indicated concentrations of unlabelled insulin (■) and H2 analogue (□). The amount of degraded radiolabelled ligand was determined by precipitation with trichloroacetic acid. Results are expressed as percentages of maximal specific degradation determined in the absence of unlabelled added peptides. (**C**) [^{125}I]Tyr^{A14}-insulin (60 fmol) was cross-linked to proteins from the cytosolic fraction (1.5 mg/ml) with 0.3 mM BS^3 at pH 7 in the absence (lanes 1, 7, 13 and 15) or presence of 1 nM to 10 μM insulin (lanes 2–6), 1 nM to 10 μM H2 analogue (lanes 8–12) or 0.1 mg/ml bacitracin (lane 14). Native cytosolic IDE was immunoprecipitated with monoclonal antibody 9B12 (lane 17) or mouse IgG (lane 16), and the supernatants were then subjected to cross-linking as described above. The arrows at the right indicate the mobility of the cross-linked insulin/IDE complex (approx. 110 kDa). The radioactive band at 66–69 kDa corresponds to radioactive BSA, which was present in the iodination mixture. The positions of molecular mass markers are shown at the left.

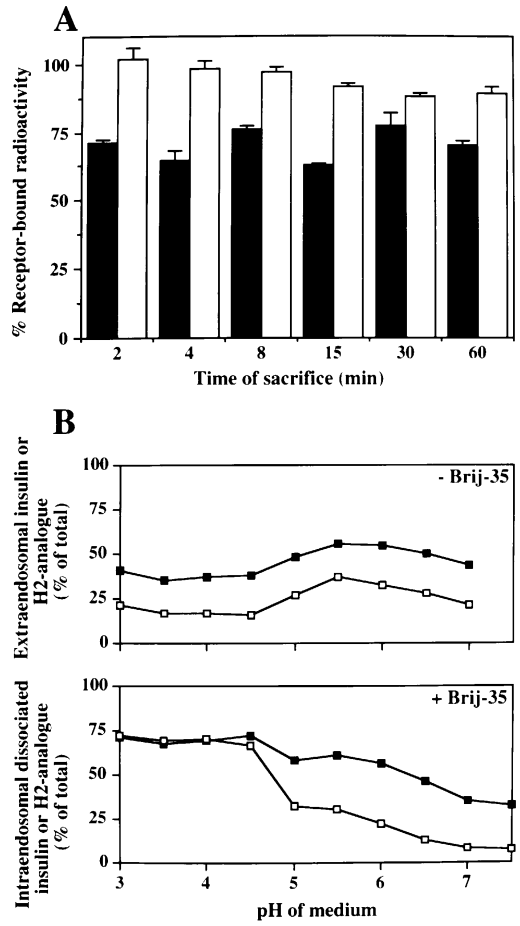

Figure 7 Dissociation states *in vivo* and *in vitro* of radiolabelled ligands within liver endosomes

(**A**) Endosomal fractions were isolated from rats killed at the indicated times after the administration of insulin (filled bars) or H2 analogue (open bars). The amount of receptor-bound radiolabelled ligands was determined by the PEG-precipitation assay in the presence of 0.1% (v/v) Brij-35. Results (mean of three to five determinations) are expressed relative to the amount of endosome-associated (PEG-precipitable in the absence of detergent) radioactivity present at zero time, which was always more than 80% of total radioactivity. (**B**) Endosomal fractions, isolated from rats killed 4 min after the injection of insulin (■) or H2 analogue (□), were incubated for 5 min in isotonic buffer at 37 °C and at different pH values, after which the incubations were supplemented with 0.15 M KCl (upper panel) or 0.1% (v/v) Brij-35 (lower panel). After a further incubation at 4 °C for 10 min, the radiolabelled ligands released from endosomes (−Brij-35) or dissociated from endosomal insulin receptor (+Brij-35) were measured by quantification of PEG-soluble radioactivity. Results (mean of three determinations) are expressed relative to the total amount of (1) radioactivity recovered in the endosomal fraction at zero time (upper panel), and (2) endosome-associated radioactivity at zero time (lower panel). The corresponding values for PEG-precipitable radioactivity with freshly prepared endosomal fractions were 82.22±0.73% for insulin and 85.08±0.81% for the H2 analogue.

[^{125}I]Tyr^{A14}-insulin degradation (Figure 6B). Insulin was found to inhibit [^{125}I]Tyr^{A14}-insulin degradation by IDE in a dose-dependent manner identical to that of the H2 analogue, with an IC_{50} of 100 nM for both molecules. Both molecules were also tested as competitors of affinity-labelling of IDE by [^{125}I]Tyr^{A14}-insulin (Figure 6C). Cross-linking of IDE was blocked by an excess (100 nM) of unlabelled insulin (Figure 6C, lane 4) as well as an excess of the H2 analogue (10^{-7} M) (lane 10). The 110 kDa band was confirmed as IDE by immunodepletion (Figure 6C, lane 17).

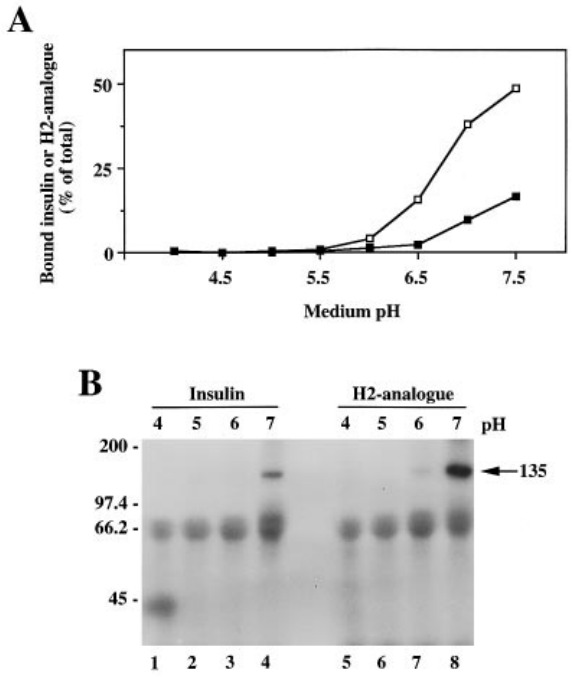

Figure 8 Binding of radiolabelled ligands *in vitro* to endosomal insulin receptor as a function of pH

(**A**) Endosomal fractions were incubated with insulin (■) or the H2 analogue (□) (9 fmol) at the indicated pH for 30–36 h, after which free and receptor-bound ligands were separated by the PEG-precipitation assay. Specific binding is expressed as a percentage of total radioactivity added, with corrections made for non-specific binding. (**B**) Ligands (60 fmol) were incubated at the indicated pH with endosomal fractions in the presence of DSS, and the fractions were subjected to SDS/PAGE. The arrow at the right indicates the mobility of the cross-linked complexes corresponding to the α-subunit of the insulin receptor (approx. 135 kDa). The radioactive band at approx. 66 kDa corresponds to radioactive BSA, which is present in the iodination mixture. The positions of molecular mass markers (in kDa) are shown at the left.

Dissociation state of intracellular radiolabelled ligands

To examine the possibility that the decreased intraendosomal degradation of the H2 analogue was due to an altered dissociation state occurring at the endosomal acidic pH, the dissociation of internalized radiolabelled ligands from the intracellular insulin receptor was studied by the PEG-precipitation protocol [9,20] (Figure 7). At any time after killing, the intraendosomal H2 analogue was more than 88% PEG-precipitable in the presence of the detergent Brij-35 (Figure 7A), suggesting that most of the analogue was receptor-bound, with dissociation from the insulin receptor virtually undetectable up to 8 min. However, the insulin recovered within endosomes over the same time period was 62–76% PEG-precipitable, suggesting that the dissociation of insulin was slightly greater than that of the H2 analogue.

The pH dependence of the dissociation of previously bound insulin and H2 analogue from endosomes was examined (Figure 7B, upper panel). The release of PEG-soluble radioactivity for both ligands was affected by pH identically to that observed for the release of trichloroacetic acid-soluble radioactivity (see Figure 4B) with a maximum at pH 5.5–6. However, over the entire range of pH, extraendosomal (PEG-soluble) radioactivity generated from insulin exceeded by approx. 2-fold that released from the H2 analogue.

To assess whether the ligands that remained associated with endosomes after incubation *in vitro* were receptor-bound or free in the endosomal lumen, the experiments described above were

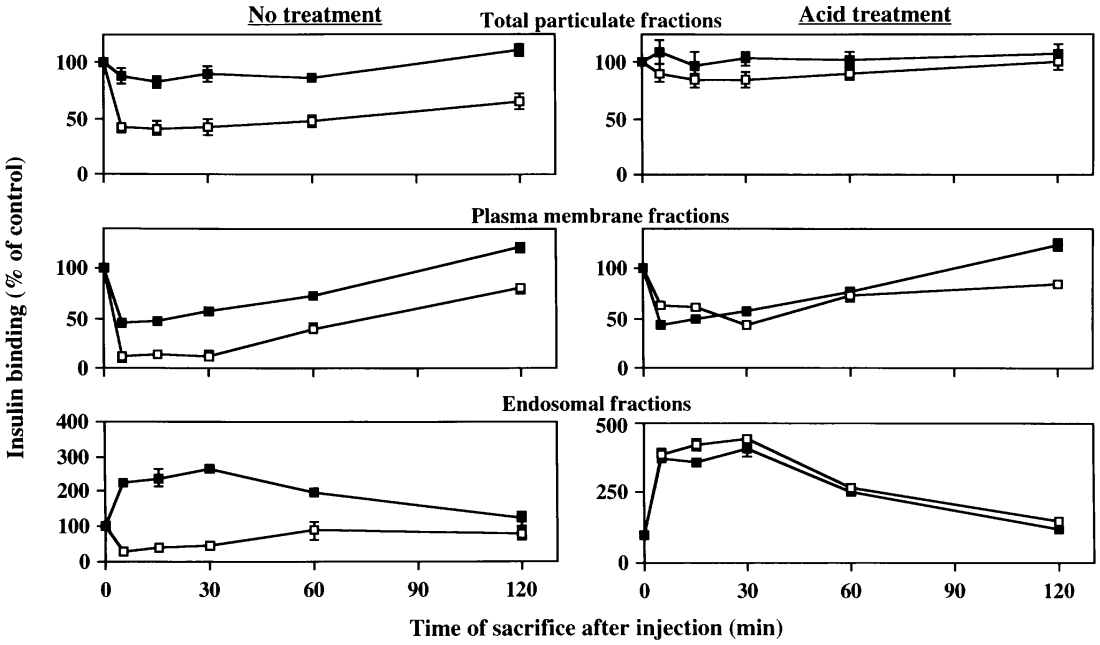

Figure 9 Changes in insulin-binding activity in liver fractions at various times after insulin or H2 analogue injection

Liver particulate, plasma membrane and endosomal fractions were isolated at the indicated times after the injection of 15 μg/100 g body weight of insulin (■) or H2 analogue (□) and examined directly for [^{125}I]Tyr^{A14}-insulin binding activity (left panels). Subcellular fractions were also depleted of endogenously bound ligands by extraction with acid and were subsequently tested for their [^{125}I]Tyr^{A14}-insulin binding activity (right panels). Results are expressed as a percentage of the insulin-binding activity in control saline-injected rats, which corresponded to: (1) no treatment, 22.02 $\pm$ 6.52 fmol/mg of protein for total particulate fractions, 116.24 $\pm$ 16.96 fmol/mg of protein for plasma membranes and 62.60 $\pm$ 6.72 fmol/mg of protein for endosomal fractions; (2) acid treatment: 14.92 $\pm$ 5.18 fmol/mg of protein for total particulate fractions, 97.76 $\pm$ 12.40 fmol/mg of protein for plasma membranes and 48.47 $\pm$ 15.89 fmol/mg of protein for endosomal fractions.

repeated with Brij-35-permeabilized endosomes (Figure 7B, lower panel). Below pH 4.5, both intraendosomal ligands were equally dissociated, with more than 70% of each ligand as free intraluminally. Between pH 4.5 and 7.5 the dissociation was more pronounced for insulin, with 33% dissociation at pH 7, whereas the solubility of the H2 analogue in PEG decreased rapidly, with less than 7% dissociation at the same pH.

Measurements were also made of the binding of each radiolabelled ligand to the endosomal insulin receptor at different pH values (Figure 8). No specific binding was detected below pH 5.5 with both the binding assay (Figure 8A) and the affinity-labelling procedure (Figure 8B, lanes 1, 2, 5 and 6). At neutral pH, specific binding of insulin was 9.7%, whereas for the H2 analogue specific binding was 37.7% (Figure 8A). A greater affinity-labelling of the insulin receptor by the H2 analogue than by insulin was confirmed at pH 7 (Figure 8B, lanes 4 and 8). Although the extent of binding of the two molecules decreased markedly at lower pH values (i.e. 6–6.5), a difference in steady-state binding between the ligands was still maintained.

H2 analogue- and insulin-induced changes in subcellular distribution of insulin-binding sites

The effect of the H2 analogue and insulin ligand occupancy *in vivo* on the kinetics and extent of insulin receptor internalization was studied with changes in the receptor content of isolated liver fractions evaluated by direct binding of [^{125}I]Tyr^{A14}-insulin (Figure 9). The administration of a single receptor-saturating dose of insulin led to a 2–2.5-fold increase in insulin-binding activity in endosomal fractions along with an approx. 50% decrease in binding activity in plasma membranes (Figure 9, left panels). These changes reached a maximum by 5–60 min, underwent reversal within 2 h and were not accompanied by major changes in binding activity in the total particulate fraction.

In contrast, the administration of the H2 analogue led to a drastic decrease (60–90%) in insulin-binding activity in the three subcellular fractions; this was maintained up to 2 h. To correct for the endogenous occupancy of binding sites by the administrated ligands [25], we developed an acid extraction procedure for endogenous receptor-bound ligands (Figure 9, right panels). A net difference was observed for fractions isolated from H2 analogue-injected rats between direct binding studies performed on freshly prepared fractions and after a low-pH extraction. Thus direct binding in the fractions, after correction for the presence of endogenous ligands, revealed for both ligands a comparable loss of binding sites from plasma membranes that coincided with entry into endosomal fractions.

To verify that the specific binding assays were representative of changes in receptor number, immunoblotting was performed with an antibody to the β subunit of the insulin receptor (Figure 10, upper panels). A time-dependent increase in receptor content was observed in endosomal fractions at 5–30 min after insulin injection, confirming the results obtained from the direct binding assay. In contrast, the level of internalized insulin receptor within endosomes after the injection of H2 analogue was more marked from 5 to 30 min, and remained elevated up to 60 min. Another difference was observed in the tyrosine phosphorylation of insulin receptor β subunit induced by the respective ligands within endosomes (Figure 10, lower panels). The administration of the H2 analogue led to a strong tyrosine phosphorylation of the insulin receptor β subunit, which was observed maximally at 5 min and was prolonged for 1 h. In contrast, insulin administration led to a brief burst (within 5 min) of tyrosine autophosphorylation of the insulin receptor.

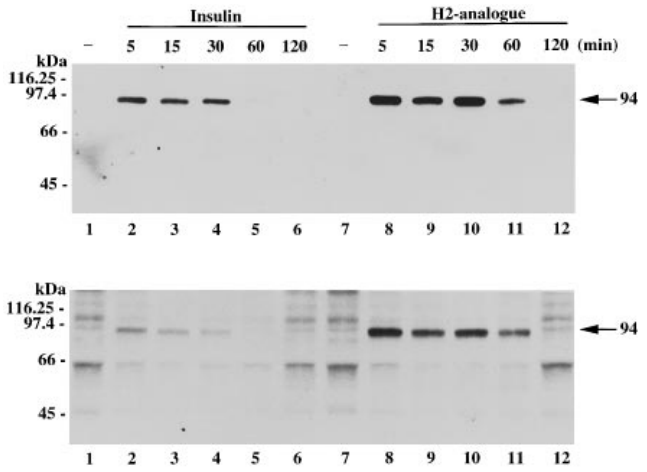

Figure 10 Kinetics of appearance of tyrosine-phosphorylated insulin receptor in endosomes after ligand administration

Endosomal fractions were isolated at the indicated times after the administration of insulin or H2 analogue (15 μg/100 g body weight) and evaluated for their content of the β subunit of the insulin receptor by using polyclonal IgG (upper panels) and for their immunoreactivity with monoclonal antibody against phosphotyrosine (lower panels). Endosomal fractions from control rats (lanes 1 and 7) were prepared from saline-injected rats killed 15 min after injection. The arrows at the right indicate the mobility of the β subunit of the insulin receptor (approx. 94 kDa). The positions of molecular mass markers are shown at the left.

DISCUSSION

The results presented here show for the first time that changing receptor affinities introduces kinetic differences in hormonal processing. The rates of organ association and elimination of the ^{123}I-labelled H2 analogue have previously been studied in rats by whole-body scintigraphy and compared with that of ^{123}I-insulin [30]. Scintigraphic recordings showed that, although both ligands reached a maximum organ association time at 4 min, the radioactive analogue slowly declined until 30 min after injection. Our experiments confirmed these findings and also showed that the altered clearance of the mutant insulin *in vivo* arises from quantitative and qualitative differences of ligand processing throughout the internalization pathway.

A difference in the handling of the H2 analogue and insulin was identified at the cell surface. A more marked association of the H2 analogue compared with insulin was observed at early times of injection at the plasma membrane level, which reflected the higher affinity of the analogue for the receptor [15,16]. A 2 min lag was required before differences in the degradation rates of both ligands were observed, a time at which the vast majority of cell-associated ligands had reached endosomal components. Hence little degradation occurred at the cell surface.

Hepatic endosomes are the major physiological locus of insulin degradation *in vivo* [2,3]. Endosomal components accumulated both radiolabelled ligands, indicating that the H2 analogue accessed the endosomal degradative compartment. That the altered clearance of the H2 analogue *in vivo* arose from decreased endosomal processing was ascribed to two different mechanisms. One was the reduced pH-dependent dissociation of the H2 analogue–receptor complexes within acidic endosomes; the second factor corresponded to the decreased ability of the free H2 analogue to be proteolysed by the endosomal acidic insulinase within the endosomal lumen.

Endosomal acidic insulinase hydrolyses insulin at a limited number of sites [12]. Although the positions of some of these cleavages are known (i.e. Leu^{A13}-Tyr^{A14}, Ala^{B14}-Leu^{B15} and Phe^{B24}-Phe^{B25}) [12], the residues of insulin important in its binding to endosomal acidic insulinase have not been defined. However, we can postulate that residues involved in the binding of insulin to the protease would be located at or near the sites at which insulin is hydrolysed by the enzyme. The amino acid substitutions in the H2 analogue did not correspond to primary sites of cleavage of insulin within endosomes. Recent studies indicate that intermediates for endosomal insulin degradation resulted from an ordered sequential pathway involving an initial cleavage in the B chain at Phe^{24}-Phe^{25} [12]. However, the replacement of amino acids near, but not within, the sites of cleavage of insulin might also significantly modify the ability of such analogues to act as effective substrates for the endosomal protease. Hence the replacement of Thr^{B27} with the more hydrophilic His residue in the H2 analogue could effectively block the Phe^{B24}-Phe^{B25} cleavage. Because the substituted amino acids in the H2 analogue have been implicated in the binding of insulin to its receptor [15,16], our results suggest that the structural determinants required for binding to receptor and endosomal acidic insulinase must differ.

Hepatic insulin processing is complicated by the postulated existence of multiple pathways for both insulin internalization and processing [2]. Therefore, despite a variety of results supporting the model in which the degradation of insulin occurs in endosomes, the quantitative role of endosomal acidic insulinase compared with that of IDE in hepatic insulin processing continues to be a subject of controversy [28,29]. The role of IDE as the physiological mediator of insulin degradation remains controversial, mainly because IDE, which displays dual peroxisomal and cytoplasmic locations, is not readily available for internalized insulin, which is located within endosomes [4,8,23,27,29,31]. The present studies provide new evidence against a role for IDE in insulin degradation in the intact cell. Both the indistinguishable rates of proteolysis and the identical order of affinities of the insulin and H2 analogue molecules for IDE do not correspond to their different susceptibilities to proteolysis by the liver *in vivo*.

The participation of the plasma membranes has also been considered in terms of cellular metabolism of the insulin hormone, but the lack of characterization of the enzyme(s) involved has prevented the evaluation of the physiological relevance of these findings [2]. The observation that part of radiolabelled insulin and H2 analogue recovered in plasma membrane fractions represents membrane-associated peptide fragments suggests that the cellular processing of each molecule is initiated at the cell surface. As described previously for the endosome-associated degradation products, the finding that the plasma membrane-associated peptide intermediates follow a different course suggests that the cellular processing of each peptide is not readily assignable to IDE. However, a neutral thiol-metalloprotease isolated from rat liver membranes represents an attractive candidate for this activity [32]. Depending on the subcellular location of the protease, this 100 kDa enzyme, structurally distinct from IDE and degrading both insulin and glucagon substrates, could have a role in the proteolytic modifications of insulin occurring on the plasma membrane surface of hepatocytes.

As the kinetics of clearance throughout liver parenchyma were dissimilar for insulin and for the H2 analogue, we pursued the possibility that a prolonged temporal interaction of a ligand with the receptor induces changes in the ligand-mediated regulation of surface receptor content and down-regulation. Injection of a saturating dose of insulin or the H2 analogue into rats caused changes in the subcellular distribution of insulin binding activity that reflect a ligand-induced endocytosis of the receptor. How-

ever, direct binding studies performed on subcellular fractions isolated from liver homogenates after administration of the H2 analogue to rats were vitiated by the content of the endogenous analogue that extensively occupied the insulin receptor throughout its internalization pathway. Only when binding assays were performed on acid-treated subcellular fractions did the receptor content change in subcellular fractions in a time- and extent-dependent fashion similar to that observed after insulin injection. These observations reinforce the view that, at the low pH that prevails in endosomes, virtually no dissociation of the H2 analogue–receptor complex occurs, leading to a larger $t_{\frac{1}{2}}$ for dissociation and a subsequent prolonged integrity state for the H2 analogue compared with insulin.

At least two other receptors associated with hepatocytes, the glucagon [19–21] and the epidermal growth factor (EGF) [33,34] receptors, have been shown to undergo translocation to the endosomal compartment after acute occupancy *in vivo* by their ligand. Although comparable with respect to their ligand-mediated internalization pathways, neither glucagon [21] nor insulin ([25], and this study) or the H2 analogue (this study) induced at saturating doses a net loss in total cellular receptors observed with total particulate fractions, a result contrasting with the data obtained with EGF [33], for which down-regulation was observed at doses of injected ligand above 50 % occupancy. However, EGF and the H2 analogue each have an extended signal transduction with a prolonged tyrosine phosphorylation of their respective receptor, occurring especially at the endosomal locus. It is noteworthy that, comparably to the H2 analogue, EGF undergoes limited proteolysis at its C-terminus within endosomes of rat liver [35], rat fibroblasts [36] and human fibroblasts [37]. Furthermore a variety of biochemical [35] and morphological [38] methods have indicated that the vast majority of EGF remains bound to its receptor in the bounding membrane of the endosome, and some proteolytic products generated within endosomes, such as EGF-(1–52), bind identically to EGF receptor and to intact EGF-(1–53) [35]. These studies, taken together with ours, indicate that within endosomes the ligand integrity and receptor-bound ligand state might influence intracellular transmembrane signalling by enhancing the autophosphorylation activity of internalized receptor kinase.

In this study we have addressed the question of why insulin and the H2 analogue seem to behave differently during receptor-mediated endocytosis into liver parenchymal cells. Thus the endosomal processing of the H2 analogue by endosomal acidic insulinase is significantly slower than that of native human insulin; the H2 analogue also has an extended duration of receptor occupancy. These results, which provide the first molecular insights into the biochemical interaction between endosomal acidic insulinase and its physiological substrate, might facilitate the design of protease-resistant insulin analogues and peptide-based inhibitors of endosomal acidic insulinase. They also support the hypothesis that the acidic protease might function in insulin signalling by degrading the insulin molecule at the endosomal locus.

We thank Dr. F. Lederer and Dr. K. H. D. Lê (UPR 9063 Centre National de la Recherche Scientifique, Gif-sur-Yvette, France) for performing N-terminal sequence analysis; Ms. P. H. Cameron (McGill University, Montreal, Quebec, Canada), for reviewing this manuscript before submission; and Dr. R. A. Roth (Stanford University, Stanford, CA, U.S.A.) for the gift of anti-IDE antibody 9B12. This work was supported by grants from the Institut National de la Santé et de la Recherche Médicale to F.A.

REFERENCES

1 Terris, S. and Steiner, D. F. (1975) J. Biol. Chem. **250**, 8389–8398
2 Authier, F., Posner, B. I. and Bergeron, J. J. M. (1994) in Cellular Proteolytic Systems (Ciechanover, A. and Schwartz, A. L., eds.), vol. 15, pp. 89–113, Wiley-Liss, New York
3 Authier, F., Posner, B. I. and Bergeron, J. J. M. (1996) FEBS Lett. **389**, 55–60
4 Authier, F., Rachubinski, R. A., Posner, B. I. and Bergeron, J. J. M. (1994) J. Biol. Chem. **269**, 3010–3016
5 Faure, R., Baquiran, G., Bergeron, J. J. M. and Posner, B. I. (1992) J. Biol. Chem. **267**, 11215–11221
6 Pease, R. J., Smith, G. D. and Peters, T. J. (1985) Biochem. J. **228**, 137–146
7 Surmacz, C. A., Wert, J. J., Ward, W. F. and Mortimore, G. E. (1988) Am. J. Physiol. **255**, C70–C75
8 Backer, J. M., Kahn, C. R. and White, M. F. (1990) J. Biol. Chem. **265**, 14828–14835
9 Pease, R. J., Smith, G. D. and Peters, T. J. (1987) Eur. J. Biochem. **164**, 251–257
10 Smith, G. D., Christensen, J. R., Rideout, J. M. and Peters, T. J. (1989) Eur. J. Biochem. **181**, 287–294
11 Desbuquois, B., Janicot, M. and Dupuis, A. (1990) Eur. J. Biochem. **193**, 501–512
12 Seabright, P. J. and Smith, G. D. (1996) Biochem. J. **320**, 947–956
13 Authier, F., Mort, J. S., Bell, A. W., Posner, B. I. and Bergeron, J. J. M. (1995) J. Biol. Chem. **270**, 15798–15807
14 Drejer, K. (1992) Diabetes-Metab. Rev. **8**, 259–286
15 Drejer, K., Kruse, V., Larsen, U. D., Hougaard, P., Bjørn, S. and Gammeltoft, S. (1991) Diabetes **40**, 1488–1495
16 Hansen, B. F., Danielsen, G. M., Drejer, K., Sørensen, A. R., Wiberg, F. C., Klein, H. H. and Lundemose, A. G. (1996) Biochem. J. **315**, 271–279
17 Lowry, O. H., Rosebrough, N. J., Farr, A. L. and Randall, R. J. (1951) J. Biol. Chem. **193**, 265–275
18 Shii, K. and Roth, R. A. (1986) Proc. Natl. Acad. Sci. U.S.A. **83**, 4147–4151
19 Authier, F., Janicot, M., Lederer, F. and Desbuquois, B. (1990) Biochem. J. **272**, 703–712
20 Authier, F. and Desbuquois, B. (1991) Biochem. J. **280**, 211–218
21 Authier, F., Desbuquois, B. and De Galle, B. (1992) Endocrinology (Baltimore) **131**, 447–457
22 Neville, D. M. (1968) Biochim. Biophys. Acta **154**, 540–552
23 Authier, F., Bergeron, J. J. M., Ou, W.-J., Rachubinski, R. A., Posner, B. I. and Walton, P. A. (1995) Proc. Natl. Acad. Sci. U.S.A. **92**, 3859–3863
24 Laemmli, U. K. (1970) Nature (London) **227**, 680–685
25 Desbuquois, B., Lopez, S. and Burlet, H. (1982) J. Biol. Chem. **257**, 10852–10860
26 Cuatrecasas, P. (1972) Proc. Natl. Acad. Sci. U.S.A. **69**, 318–322
27 Authier, F., Cameron, P. H. and Taupin, V. (1996) Biochem. J. **319**, 149–158
28 Becker, A. B. and Roth, R. A. (1995) Methods Enzymol. **248**, 693–703
29 Authier, F., Posner, B. I. and Bergeron, J. J. M. (1996) Clin. Invest. Med. **19**, 149–160
30 Jensen, I., Kruse, V. and Larsen, U. D. (1991) Diabetes **40**, 628–632
31 Kuo, W.-L., Gehm, B. D., Rosner, M. R., Li, W. and Keller, G. (1994) J. Biol. Chem. **269**, 22599–22606
32 Blache, P., Kervran, A., Le-Nguyen, D., Dufour, M., Cohen-Solal, A., Duckworth, W. and Bataille, D. (1993) J. Biol. Chem. **268**, 21748–21753
33 Lai, W. H., Cameron, P. H., Wada, I., Doherty, J. J., Kay, D. G., Posner, B. I. and Bergeron, J. J. M. (1989) J. Cell Biol. **109**, 2741–2749
34 Jäckle, S., Runquist, E. A., Miranda-Brady, S. and Havel, R. J. (1991) J. Biol. Chem. **266**, 1396–1402
35 Renfrew, C. A. and Hubbard, A. L. (1991) J. Biol. Chem. **266**, 4348–4356
36 Planck, S. R., Finch, J. S. and Magun, B. E. (1984) J. Biol. Chem. **259**, 3053–3057
37 Wiley, H. S., VanNostrand, W., McKinley, D. N. and Cunningham, D. D. (1985) J. Biol. Chem. **260**, 5290–5295
38 Carpentier, J.-L., White, M. F., Orci, L. and Kahn, C. R. (1987) J. Cell Biol. **105**, 2751–2762

Received 5 January 1998/20 February 1998; accepted 11 March 1998